Improved Regrowth Interface of AlGaInAs/InP-Buried-Heterostructure Lasers by *In-Situ* Thermal Cleaning

Yuta Takino, Mizuki Shirao, *Member, IEEE*, Noriaki Sato, Takashi Sato, Tomohiro Amemiya, *Member, IEEE*, Nobuhiko Nishiyama, *Senior Member, IEEE*, and Shigehisa Arai, *Fellow, IEEE*

***Abstract*— The influence of *in-situ* thermal cleaning on the regrowth interface quality of 1.3-μm wavelength AlGaInAs/InP-buried-heterostructure (BH) lasers grown by organo-metallic vapor-phase epitaxy was investigated. The surface recombination velocity estimated from below threshold electroluminescence measurements was used to quantitatively study regrowth interface quality. The relationship between surface recombination velocity and lasing properties was supported by theory. In this way, we could validate the use of surface recombination velocity as a measure of interface quality. *In-situ* thermal cleaning at 650 °C for 45 min under PH_3 atmosphere resulted in operational BH lasers (1.6 μm stripe width) with a differential quantum efficiency of 66% and an internal quantum efficiency of approximately 76%.**

***Index Terms*— AlGaInAs/InP, buried-heterostructure, organo-metallic vapor-phase epitaxy, thermal cleaning.**

I. Introduction

AlGaInAs/InP 1.3-μm band semiconductor lasers have been extensively studied for subscriber loop applications due to their high performance operation at higher temperatures than GaInAsP/InP based semiconductor lasers [1]–[7]. The larger conduction band offset ($\Delta E_c = 0.75\ \Delta E_g$) for the AlGaInAs/InP alloy system compared to that of the GaInAsP/InP system ($\Delta E_c = 0.40\ \Delta E_g$) [8] enables high performance operation in a wider temperature range. Transmitter modules can then be built without thermoelectric coolers, lowering both cost and power consumption. Since the AlGaInAs/InP alloy system also has a potentially higher material and differential gain [9], [10], high speed direct modulation and electro-absorption modulator integrated distributed feedback lasers were realized [11]–[17].

For stripe geometry lasers used in optical fiber communications, the buried-heterostructure (BH) was frequently adopted due to its low operating current, stable output beam pattern, and high-speed operation compared with a ridge waveguide structure [5], [12]–[14], [16], [18]–[21]. However, the oxidation of Al-containing layers made the adoption of BH structures using the AlGaInAs/InP system difficult. Such oxidation caused a degradation of crystal quality during the embedding growth process and subsequently resulted in poor lasing characteristics and low reliability [7], [13]. In order to overcome this problem, various processes that prevent oxidation or remove the oxidized surface of Al-containing layers have been reported. Some of these methods are listed in Table I.

While these methods were reported to overcome the oxidation problem, quantitative studies of the regrowth interface quality in BH structures have not been reported. We have previously examined an *in-situ* thermal cleaning process for the AlGaInAs/InP BH laser, focusing on the cleaning time [23] and temperature [24]. Regrowth interface quality was evaluated using the surface recombination velocity estimated from the electroluminescence slope efficiency below the threshold current. By adopting this process, room-temperature continuous-wave (RT-CW) operation of a AlGaInAs/InP transistor laser emitting at a 1.3 μm wavelength was successfully obtained [23], [24].

In this paper, we report a comprehensive study on in-situ thermal cleaning for AlGaInAs/InP-BH laser and achieve better characteristics than in our and other's previous reports on such lasers. In addition, the quantitative theoretical analysis, with derivation of the formula for the surface recombination velocity, is also mentioned. In Section II, the fabrication processes and *in-situ* thermal cleaning conditions used in this study are explained. We also provide a method for evaluating regrowth interface quality using surface recombination velocity measurements. Section III is devoted to the relationship between surface recombination velocity and regrowth interfaces under three conditions: cleaning time, atmosphere, and cleaning temperature. The surface recombination velocity of AlGaInAs/InP BH lasers obtained under the best thermal cleaning conditions is compared with that of GaInAsP/InP

Manuscript received December 9, 2011; revised April 9, 2012; accepted April 12, 2012. Date of publication April 25, 2012; date of current version May 15, 2012. This work was supported in part by the Ministry of Education, Culture, Sports, Science and Technology, Japan, and the Japan Society for Promotion of Science under Grants-in-Aid for Scientific Research under Grant 19002009, Grant 21226010, Grant 22360138, Grant 21860031, and Grant 10J09593.

Y. Takino, M. Shirao, N. Sato, T. Sato, and N. Nishiyama are with the Department of Electrical and Electronic Engineering, Tokyo Institute of Technology, Tokyo 152-8552, Japan (e-mail: takino.y.aa@m.titech.ac.jp; shirao.m.aa@m.titech.ac.jp; sato.n.ad@m.titech.ac.jp; sato.t.af@m.titech.ac.jp; n-nishi@pe.titech.ac.jp).

T. Amemiya and S. Arai are with the Quantum Nanoelectronics Research Center, Tokyo Institute of Technology, Tokyo 152-8552, Japan (e-mail: amemiya.t.ab@m.titech.ac.jp; arai@pe.titech.ac.jp).

Color versions of one or more of the figures in this paper are available online at http://ieeexplore.ieee.org.

Digital Object Identifier 10.1109/JQE.2012.2196410

0018–9197/$31.00 © 2012 IEEE

TABLE I
LIST OF PREVIOUS STUDIES ON EMBEDDING REGROWTH FOR THE AlGaInAs MATERIAL SYSTEM

Purposes	Methods	Ref.
Interference with the oxidation	Narrow-stripe selective organo-metallic vapor-phase-epitaxy (NS-OMVPE)	[13], [21]
	Passivation by the NH_4S solution	[22]
	Minimization of the exposure time between the etching and the regrowth	[12]
Disposal of the oxidized surface	Heating under phosphine pressure prior to the growth	[12]
	Treatment by HF solution	[5]
	In-situ etching at the OMVPE reactor prior to the regrowth	[19], [20]

BH lasers fabricated under the same conditions. Finally, we conclude this study in Section IV.

II. Fabrication Process and Thermal Cleaning Condition

A. Fabrication Process With Thermal Cleaning

The initial wafer consists of (a) a 500 nm thick n-InP cladding layer, (b) a 30 nm thick n-AlInAs layer, (c) a bottom 100 nm thick n-AlInAs to u-AlGaInAs graded-index separate confinement heterostructure (GRIN-SCH) layer, (d) five $Al_{0.15}Ga_{0.12}In_{0.73}As$ quantum wells (QWs), 5 nm thick, compressively strained (CS) by 1.4%, which comprise the active layer for 1.3 μm wavelength laser light, (e) six 10 nm thick t0.7% tensile-strained (TS) $Al_{0.25}Ga_{0.32}In_{0.43}As$ barrier layers, (f) an upper 100 nm thick u-AlGaInAs to p-AlInAs GRIN-SCH layer, (g) a 30 nm thick p-AlInAs layer, a 30 nm thick p-InP layer, and a 30 nm thick GaInAs layer. These layers were grown on a (100) n-InP substrate using a low pressure (0.1 atm) OMVPE technique.

Mesa stripes were formed from a combination of wet and dry etching using a SiO_2 mask with various widths. Firstly, the GaInAs and Al-containing layers (about 450 nm thick) were etched using a bromine-methanol solution (Br_2/CH_3OH = 1:1000) in order to reach the n-InP cladding layer. Since this solution gives isotropic etching, the actual mesa stripes narrowed by approximately 1.4–1.5 μm compared to the initial width of the SiO_2 mask. Next, an additional depth of 300 nm was reached by CH_4/H_2 reactive ion etching (RIE). Wet cleaning was then carried out by 3 steps by using Br_2/CH_3OH = 1:40000, $H_2SO_4/H_2O_2/H_2O$ = 1:1:40, and 1% BHF. The 1st step was for removing the dry etching damage, the 2nd step was for treatment of the active region and the last step was for removing of the oxidized layer on the whole surface and the Al-containing region. The wafer was then immediately loaded into the OMVPE reactor and thermal cleaning was carried out prior to the growth of the current blocking layers. Thermal cleaning was conducted under various conditions by changing the time, atmosphere, and temperature, which will be explained in Section III. Wafer loading time can affect regrowth interface quality. We found

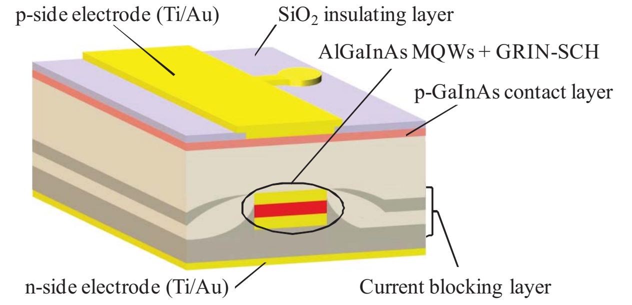

Fig. 1. Structure of the fabricated BH lasers.

that device characteristics degraded dramatically for wafer loading times of over 60 min. We set the exposure time to within 4 min, since no changes occurred in this time. After loading, the wafer underwent regrowth of the 100 nm thick n-InP current blocking layers, the 200 nm thick p-InP layers, and the 300 nm thick n-InP layers. These layers were selectively grown in order to bury the mesa stripes. After removing the SiO_2 mask and the GaInAs layer, a second regrowth of (h) a 1.6 μm thick p-InP cladding layer and (i) a 50 nm thick p^+-GaInAs contact layer was carried out.

After polishing the back side of the wafer to a thickness of 100–150 μm, Ti/Au electrodes were evaporated onto both sides of the wafer and facets were formed by cleavage for laser cavities. The structure of the fabricated AlGaInAs/InP BH laser is shown in Fig. 1 and the final structure of the laser is shown in Table II.

B. Evaluation of Surface Recombination Velocity

In order to evaluate the quality of the regrowth interface, we introduced a non-radiative recombination rate at the sidewall. This is the so-called surface recombination velocity S [25] estimated from the following relation (see Appendix),

$$\frac{\eta_{\mathrm{spon,BH}}}{\eta_{\mathrm{spon,BHO}}} = 1 - \frac{\frac{2S\cdot\tau}{W-2W_{\mathrm{d}}}}{1+\frac{S\cdot\tau}{L_{\mathrm{D}}}\coth\left\{(\mathrm{W}-2\mathrm{W_d})/2\mathrm{L_D}\right\}} \quad (1)$$

where $\eta_{\mathrm{spon,BH}}$ is the spontaneous emission efficiency at a low injection current level, τ is the carrier lifetime of the BH structure when $S = 0$, L_D is the diffusion length of electrons, which is 5 μm for intrinsic AlGaInAs, and W is the stripe width. Equation (1) involves carrier diffusion since W is as wide as L_D and can be rewritten as (2) when W is very narrow compared to the carrier diffusion length and the carrier density can be regarded as constant [25]–[29].

$$\frac{\eta_{\mathrm{spon,BH}}}{\eta_{\mathrm{spon,BHO}}} = \frac{1}{1+\frac{2S\bullet\tau}{W-2W_{\mathrm{d}}}}. \quad (2)$$

Thus, W_d is the "dead layer thickness" as shown in Fig. 2. However, in this report, we have assumed W_d to be negligible in comparison to the stripe width, $W \gg W_d$, because when considered to be a lattice defect region due to the oxidation of Al-containing layers, W_d was found to be very thin from our cross sectional SEM and TEM measurements (Fig. 3). Furthermore, $\eta_{\mathrm{spon,BH0}}$ is the spontaneous emission efficiency of the BH laser with a broad stripe width for normalization.

TABLE II
LIST OF THE LAYERS OF THE LASER STRUCTURE

Contents	Material	λ_g [μm]	N_D [cm^{-3}]	d [μm]	$T_{\rm growth}$ [°C]
(i) Contact layer	p^+-$Ga_{0.47}In_{0.53}As$	1.65	1.0×10^{19}	0.050	600
(h) Upper cladding layer	p-InP	0.92	5.0×10^{17}	1.600	650
(g) Upper n-SCH	p- $Al_{0.47}In_{0.53}As$	0.81	2.0×10^{17}	0.030	700
(f) Upper n-GRIN-SCH ↑ Upper u-GRIN-SCH	p- $Al_{0.47}In_{0.53}As$ ↑ u- $Al_{0.27}Ga_{0.20}In_{0.53}As$	0.81 ↑ 1.07	2.0×10^{17} ↑ -	p-0.070 u-0.030	700
(e) TS -0.7% barrier layer ×5	u- $Al_{0.22}Ga_{0.35}In_{0.43}As$	1.07	-	0.010	700
(d) CS 1.4% well layer ×5	u- $Al_{0.17}Ga_{0.10}In_{0.73}As$	1.50	-	0.005	700
TS -0.7% barrier layer	u- $Al_{0.22}Ga_{0.35}In_{0.43}As$	1.07	-	0.010	700
(c) Bottom u-GRIN-SCH ↑ Bottom n-GRIN-SCH	u- $Al_{0.27}Ga_{0.20}In_{0.53}As$ ↑ n- $Al_{0.47}In_{0.53}As$	1.07 ↑ 0.81	- ↑ 1.0×10^{17}	u-0.005 n-0.095	700
(b) Bottom n-SCH	n- $Al_{0.47}In_{0.53}As$	0.81	1.0×10^{17}	0.030	700
(a) Bottom cladding layer	n-InP	0.92	1.0×10^{18}	0.500	650
Substrate	n-InP	0.92	5.0×10^{18}	350	650

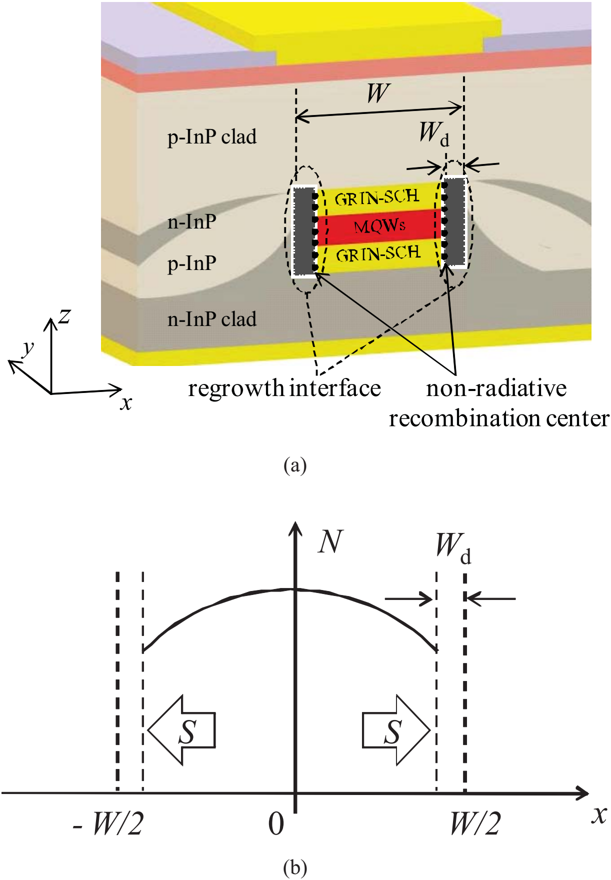

Fig. 2. (a) Cross-sectional structure. (b) Model of carrier density profile around active region.

(48.6 μm was used in this case). If there were no non-radiative recombination centers at the regrowth interface, which corresponds to $S{\cdot}\tau = 0$, the normalized spontaneous emission efficiency $\eta_{\rm spon,BH}/\eta_{\rm spon,BH0}$ should approach 1 even for a narrow stripe width. The normalized spontaneous emission efficiency curves for various $S{\cdot}\tau$ values are plotted in Fig. 4.

III. MEASUREMENT RESULTS

A. Cleaning Time Dependence

We first investigated how the spontaneous emission efficiency of BH lasers with various stripe widths varied with thermal cleaning time at a fixed reactor temperature of 450°C and PH_3 atmosphere. Thermal cleaning time periods of 15, 30, 45, 60, and 90 min were used. The PH_3/H_2 gas flow rate was kept at 300/5000 sccm, which was also used for the growth of InP and GaInAsP crystals in our OMVPE system.

Fig. 5 shows RT-CW light output characteristics of AlGaInAs/InP BH lasers for various stripe widths with a 500 μm cavity length fabricated using a thermal cleaning time of 30 min. The lasing wavelength was around 1.34 μm for all devices except for the device with $W = 48.6$ μm, which did not operate under RT-CW conditions. While the threshold current reduced with decreasing stripe width down to $W = 1.6$ μm, it increased for $W = 0.6$ μm with a drastically reduced differential quantum efficiency η_d. The increase of the threshold current can be attributed to an increase in the ratio of non-radiative recombination current to total injection current. The decrease of η_d can be attributed to an increase of an absorption loss (inter valence band absorption: IVBA) and/or heat generation because these devices were not bonded to heat sinks. In order to evaluate the spontaneous emission efficiency of these devices, we measured the light output characteristics far below the threshold ($I < 5$ mA) as shown in Fig. 6. Light output increased almost linearly with the injection current for all devices, which means that amplification of spontaneous emission is negligible and so the incremental slope of light output to injection current is a measure of the internal quantum efficiency. The considerable decrease in slope efficiency

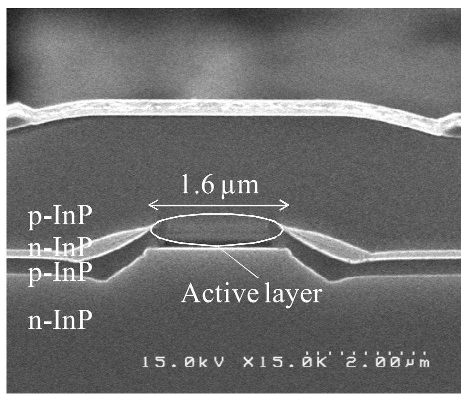

(a)

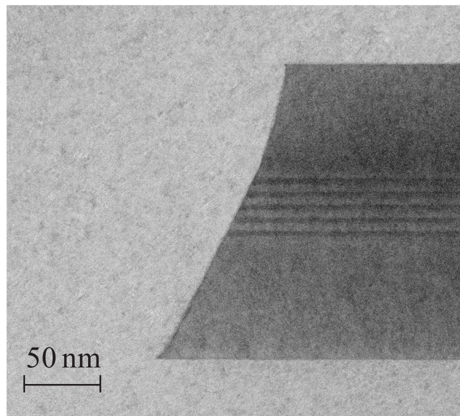

(b)

Fig. 3. Cross-sectional (a) SEM and (b) TEM views for lasers fabricated by the thermal cleaning conditions of 45 min in PH_3 atmosphere at 650 °C.

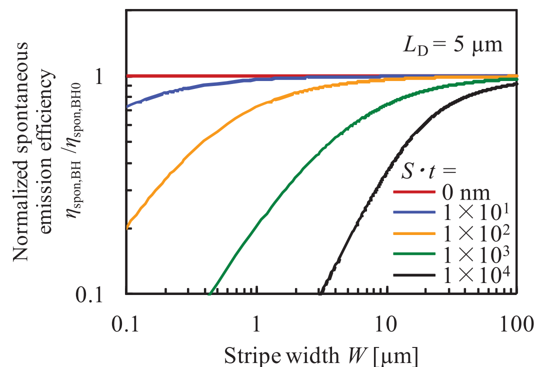

Fig. 4. Normalized spontaneous emission efficiency for various values of S·τ product as a function of the stripe width.

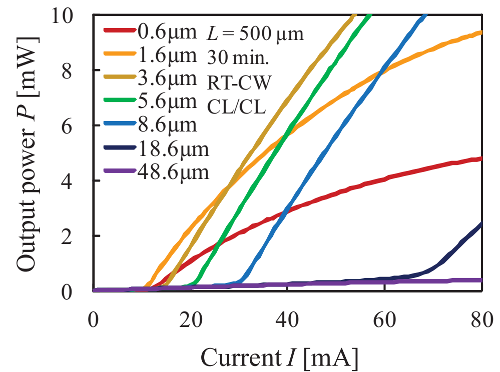

Fig. 5. Light output characteristics of AlGaInAs/InP BH lasers with various stripe widths fabricated by thermal cleaning conditions of 30 min in PH_3 atmosphere at 450 °C.

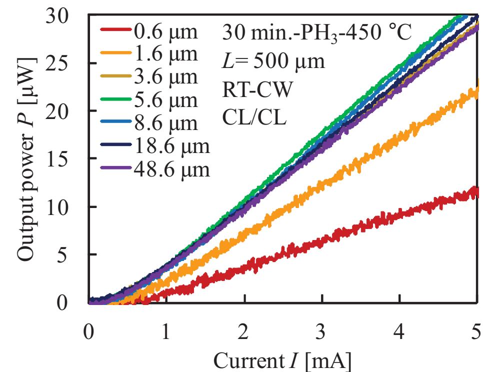

Fig. 6. Light output characteristics below 30 μW of AlGaInAs/InP BH lasers with various stripe widths fabricated by thermal cleaning conditions of 60 min in PH_3 atmosphere at 450 °C.

for stripe widths of less than 1.6 μm can be attributed to non-radiative recombination at the regrowth interface.

Fig. 7 shows the normalized spontaneous emission efficiency of BH lasers $\eta_{\mathrm{spon,BH}}/\eta_{\mathrm{spon,BH0}}$ as a function of the stripe width for various thermal cleaning times at a fixed 500 μm cavity length. From this data and (1), the $S{\cdot}\tau$ product was estimated by the least-square method to be 619 (poor fitting), 307, 315, 343, and 1723 nm for cleaning time periods of 15, 30, 45, 60, and 90 min, respectively. However, for the 15 min cleaning process, $\eta_{\mathrm{spon,BH}}/\eta_{\mathrm{spon,BH0}}$ did not reach 1 even for wide stripe (e.g., 8.6 μm or 18.6 μm) samples because of the large non-radiative recombination components observed at both the side walls and throughout the stripe. Thus, a clear improvement was observed for a cleaning time range of 30 to 60 min compared with 15 and 90 min.

B. Cleaning Atmosphere

Since an introduction of PH_3 gas prior to the crystal growth of GaInAsP/InP compounds in OMVPE is usually used to prevent the desorption of phosphorus from the surface of the P-containing substrate/wafer, we mostly investigated thermal cleaning under PH_3 atmosphere. However, in the AlGaInAs compound system the group V material is As and so we tried AsH_3 as the atmosphere. Using the results of section III-*A*, the cleaning time and the temperature were fixed at 45 min and 450°C, respectively. The gas flow rate of AH_3/H_2 was kept at 46.2/5254 sccm, which was the same as that used for the growth of AlGaInAs crystals in our OMVPE system.

The normalized spontaneous emission efficiency of BH lasers as a function of the stripe width under these conditions is shown in Fig. 8. The $S{\cdot}\tau$ product was 315 and 1033 nm for PH_3 and AsH_3 atmospheres, respectively. PH_3 was found to be more effective even for regrowth on AlGaInAs crystals in our OMVPE system. Furthermore, the $S{\cdot}\tau$ value obtained with this condition (45 min under AsH_3 atmosphere) was larger relative to that obtained for 15 min under PH_3 atmosphere and this shows that the regrowth interface quality of the device with the

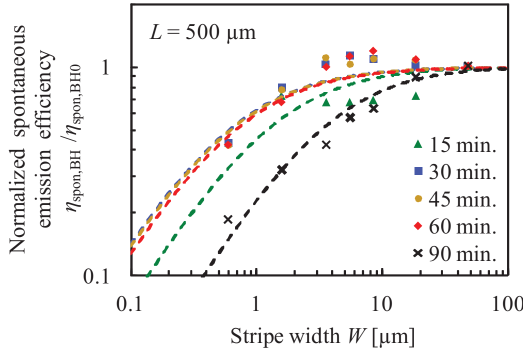

Fig. 7. Stripe width dependence of normalized spontaneous emission efficiency for the thermal cleaning at 450 °C under PH_3 atmosphere.

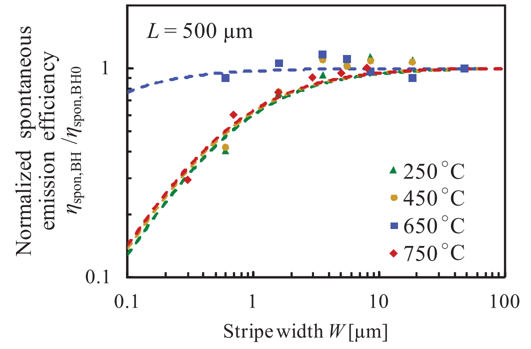

Fig. 9. Stripe width dependence of normalized spontaneous emission efficiency for a thermal cleaning time of 45 min under PH_3 atmosphere.

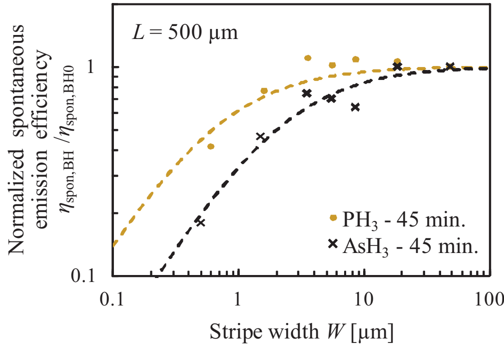

Fig. 8. Stripe width dependence of normalized spontaneous emission efficiency for thermal cleaning at 450 °C for 45 min.

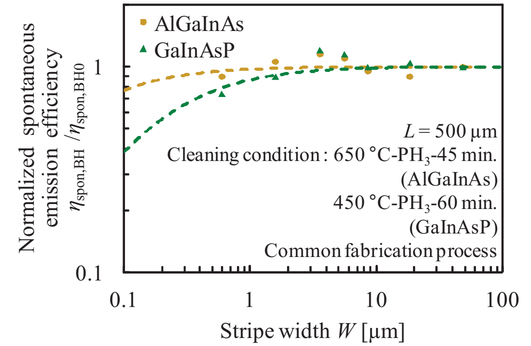

Fig. 10. Stripe width dependence of normalized spontaneous emission efficiency for AlGaInAs/InP and GaInAsP/InP BH lasers fabricated with a thermal cleaning under PH_3 atmosphere at 650 °C for 45 min and 450 °C for 60 min, respectively.

condition of AsH_3 for 45 min is inferior to that of PH_3 for 15 min. Several reasons can be considered for this phenomenon. (1) PH_3 reacts with AlGaInAs to form AlGaInAsP with PH_3 penetrating the porous very thin AlO film on the surface and this higher bandgap AlGaInAsP keeps carriers away from the surface. (2) Oxygen atoms in Al-O bonds were replaced by phosphorus atoms for the PH_3 flow, although further chemical equilibrium analysis is required to determine the extent of this reaction in the present experiment.

In addition, too long cleaning time periods such as 90 min. degrade the quality of quantum wells and exposed surfaces due to too much desorption of atoms and intermixing.

C. Cleaning Temperature Dependence

The dependence of regrowth interface quality on thermal cleaning temperature was investigated for various cleaning temperatures at a fixed 45 min cleaning time and PH_3 atmosphere. Fig. 9 shows the normalized spontaneous emission efficiency of BH lasers as a function of the stripe width for various thermal cleaning temperatures at a fixed 500 μm cavity length. The $S{\cdot}\tau$ product was estimated to be 344, 315, 15, and 302 nm for cleaning temperatures of 250, 450, 650, and 750 °C, respectively. Remarkably, thermal cleaning at 650°C resulted in the highest normalized spontaneous emission efficiency, achieving better regrowth interface quality.

In a previous report [30], the thermal decomposition of PH_3 was found to increase at a temperature higher than 450°C. At 650°C, the quality of the regrown interfaces was improved most efficiently in terms of the reaction of atoms. However, much higher temperatures, such as 750°C, degraded crystal quality of AlGaInAs and GaInAsP due to the desorption of As and P. From our experimental results, a thermal cleaning temperature of 650°C was found to be an optimal condition.

D. Surface Recombination Velocity in AlGaInAs/InP and GaInAsP/InP BH Lasers and Cleaning Temperature Dependence

Generally, the GaInAsP/InP system is less susceptible to oxidation compared to the AlGaInAs/InP system. However a direct comparison of the $S{\cdot}\tau$ product between these systems has not been reported yet. We fabricated GaInAsP/InP BH lasers (1.55 μm lasing wavelength) using the same etching, wet cleaning, and regrowth processes used for AlGaInAs/InP BH lasers are shown in Fig. 10. Please note two alloy systems have difference optimum thermal cleaning conditions. The previously reported $S{\cdot}\tau$ product for GaInAsP/InP quantum wire lasers was around 3 nm [27]. The lower $S{\cdot}\tau$ product in quantum wire structures may be attributed to the difference in the 130 nm etched mesa height compared to the 1 μm height for the BH stripe.

E. Lasing Properties

Finally, we measured the light output characteristics of AlGaInAs/InP BH lasers with various cavity lengths. We compared the cavity length dependences of the threshold current I_{th} and the external differential quantum efficiency η_d.

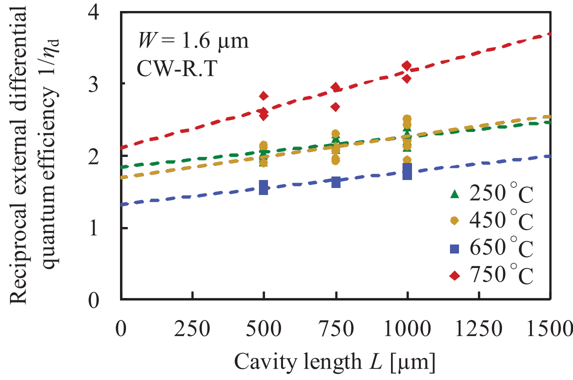

Fig. 11. Reciprocal external quantum efficiency of AlGaInAs/InP BH lasers as a function of the cavity length for $W = 1.6\ \mu$m fabricated with a thermal cleaning time of 45 min under PH_3 atmosphere.

TABLE III
LIST OF THERMAL CLEANING CONDITION LASING CHARACTERISTICS FOR 45 MIN UNDER PH_3 ATMOSPHERE, WITH $L = 500\ \mu$m

Cleaning Temperature [°C]	η_i [%]	α [cm^{-1}]	$S{\cdot}\tau$ [nm]
250	55	3	344
450	59	4	315
650	76	4	15
750	48	6	302

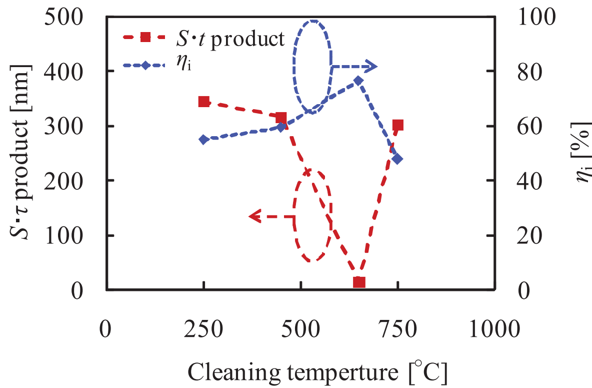

Fig. 12. Cleaning temperature dependence of S·τ product and internal quantum efficiency for $W = 1.6\ \mu$m fabricated with a thermal cleaning time of 45 min under PH_3 atmosphere.

Under the thermal cleaning conditions of 45 min under PH_3 at 650°C, the lowest threshold current of $I_{th} = 8.1$ mA (threshold current density $J_{th} = 1.0$ kA/cm^2) and highest external differential quantum efficiency of $\eta_d = 66\%$ was obtained for a stripe width of $W = 1.6\ \mu$m and a cavity length of $L = 500\ \mu$m. These values are comparable to or even better than those reported for AlGaInAs/InP BH lasers [5], [13]. Fig. 11 shows the cavity length dependence of the inverse of η_d (both facets) for various thermal cleaning temperatures. In Fig. 11, the y-intercept and slope were used to estimate, the internal quantum efficiency η_i and waveguide loss α, respectively, in Table III. α was less sensitive to the cleaning temperature except at 750°C.

Fig. 12 shows the cleaning temperature dependence of the internal quantum efficiency η_i and the $S{\cdot}\tau$ product. The $S{\cdot}\tau$ product was drastically reduced while the highest η_i was attained at a cleaning temperature of 650°C. From the comparison of the η_i and the $S{\cdot}\tau$ product, a lower $S{\cdot}\tau$ product leads to better lasing characteristics, though better lasing characteristics need not lead to a better $S{\cdot}\tau$ product. Even so, since an appropriate thermal cleaning condition leads to higher internal quantum efficiency consistent with the cleaning condition for the lowest $S{\cdot}\tau$ product, our approach to evaluate the sidewall recombination velocity is effective for improving lasing characteristics of AlGaInAs/InP BH lasers.

IV. CONCLUSION

In conclusion, AlGaInAs/InP BH lasers emitting at a 1.3 μm wavelength were fabricated under various thermal cleaning conditions prior to the embedding growth. The regrowth interface quality for different thermal cleaning conditions was quantitatively evaluated in terms of the product of the non-radiative recombination velocity and the carrier lifetime. We found that a PH_3 atmosphere gave better regrown interfaces than an AsH_3 atmosphere. A thermal cleaning temperature of 650°C over a period of 45 min gave the best lasing characteristics for a five quantum well AlGaInAs/InP BH laser. The best thermal cleaning process resulted in a typical threshold current of 8.1 mA and differential quantum efficiency of 66% for a 1.6 μm stripe width and 500 μm cavity length. An internal quantum efficiency as high as 76% was obtained under the same thermal cleaning conditions. A good correlation between low non-radiative recombination velocity and high performance lasing characteristics was experimentally confirmed.

V. APPENDIX

Equations (A.7) and (A.9) can be derived as follows. Firstly, the rate equation for the carrier density in the active region is expressed as,

$$\frac{\partial N(x,t)}{\partial t} = D\frac{\partial^2 N(x,t)}{\partial x^2} - \frac{N(x,t)}{\tau} + G \quad \text{(A.1)}$$

where D is the diffusion constant of carriers, τ is the carrier lifetime, and G is the injected carrier density per unit time. Here only the dependence on the stripe width direction (x-axis) was considered for simplicity as shown in Fig. 2(b). The surface recombination behavior is given by the definition of surface recombination velocity as

$$\pm D\frac{\partial N(x,t)}{\partial x} = -S \cdot N(x,t)$$
$$\text{at } x = \pm(W/2 - W_d) = \pm A. \quad \text{(A.2)}$$

At steady state, ∂ / ∂t = 0, (A.1) reduces to

$$\frac{\partial^2 N(x,t)}{\partial x^2} = \frac{N(x,t)}{\tau \cdot D} - \frac{G}{D}, \quad \text{(A.3)}$$

and (A.3) can be solved by using the boundary conditions given by (A.2),

$$N(x,t) = \tau \cdot G - \frac{S \cdot \tau^2 \cdot G}{2\left(L_D \sinh(A/L_D) + S \cdot \tau \cosh(A/L_D)\right)} \cosh(x/L_D) \quad \text{(A.4)}$$

where L_D is the diffusion length, and $L_D^2 = D\tau$. The two dimensional carrier density M [cm^{-2}] in the x direction is given by

$$M = \int_{-A}^{A} N(x)dx \times \tau \cdot G \cdot A - \frac{S \cdot \tau^2 \cdot G}{L_{\mathrm{D}}\sinh(A/L_{\mathrm{D}}) + S \cdot \tau\cosh(A/L_{\mathrm{D}})} \times L_{\mathrm{D}}\sinh(A/L_{\mathrm{D}}). \quad (A.5)$$

Using (A.5), we can estimate S but a direct measurement of the total number of carriers in the active region is difficult. Thus, in this paper we used the spontaneous efficiency η_{spon}, which is the output power efficiency at low current injection level with only spontaneous radiation, in order to estimate S under the assumption that the non-radiative recombination factor is independent of stripe width except for surface recombination.

Next, we will expand M in (A.5) in order to obtain an expression for η_{spon}. When the stripe width is very wide and the surface recombination at sidewalls can be negligibly small, M can be rewritten as M_0.

$$M_0 = \tau \cdot G \cdot A. \quad (A.6)$$

Then the total number of carriers in the active region can be computed by multiplyingM_0 the active region thickness d, and the cavity length L. The spontaneous emission efficiency of a BH laser with a stripe width W normalized by that with a very wide stripe width is

$$\frac{\eta_{\mathrm{spon,BH}}}{\eta_{\mathrm{spon,BH0}}} = \frac{\frac{M \cdot d \cdot L}{\tau_R + \tau_{NR}}}{\frac{M_0 \cdot d \cdot L}{\tau_R + \tau_{NR}}} = 1 - \frac{\frac{S \cdot \tau}{A}}{1 + \frac{S \cdot \tau}{L_D}\coth\left(A/L_D\right)}. \quad (A.7)$$

The power series expansion around A of coth(A/L_D) can be written as,

$$\coth x = \frac{1}{x} + \frac{x}{3} - \frac{x^3}{45} + \frac{2x^5}{945} + = \frac{1}{x} + \sum_{n=1}^{\infty} \frac{2^{2n} B_{2n} x^{2n-1}}{(2n)!} \quad \text{for} \quad 0 < |x| < \pi \quad (A.8)$$

where B_n is the Bernoulli number. When the stripe width is very narrow compared with L_D as in quantum wire structures [26]–[28], only the first term is picked up and (A.7) can be rewritten as,

$$\frac{\eta_{\mathrm{spon,BH}}}{\eta_{\mathrm{spon,BH0}}} = 1 - \frac{\frac{S \cdot \tau}{A}}{1 + \frac{S \cdot \tau}{L_D} \cdot \frac{L_D}{A}} = \frac{1}{1 + \frac{S \cdot \tau}{A}}, \quad A \equiv \frac{W}{2} - W_d. \quad (A.9)$$

Acknowledgment

We would like to thank E. Y. Suematsu, K. Iga, K. Furuya, and K. Kobayashi, for continuous encouragement, and M. Asada, F. Koyama, T. Mizumoto, Y. Miyamoto, M. Watanabe, T. Miyamoto, H. Uenohara, and S. Akiba, at the Tokyo Institute of Technology, Tokyo, Japan, for fruitful discussions.

References

[1] C. E. Zah, R. Bhat, B. N. Pathak, F. Favire, W. Lin, M. C. Wang, N. C. Andreadakis, D. M. Hwang, M. A. Koza, T. P. Lee, Z. Wang, D. Darby, D. Flanders, and J. J. Hsieh, "High-performance uncooled 1.3-μm $\mathrm{Al_xGa_yIn_{1-x-y}As}$/InP strained-layer quantum-well lasers for subscriber loop applications," *IEEE J. Quantum Electron.*, vol. 30, no. 2, pp. 511–523, Feb. 1994.

[2] R. F. Kazarinov and G. L. Belenky, "Novel design of AlGaInAs-InP lasers operating at 1.3 μm," *IEEE J. Quantum Electron.*, vol. 31, no. 3, pp. 423–426, Mar. 1995.

[3] J. Pan and J. Chyi, "Theoretical study of the temperature dependence of 1.3 μm AlGaInAs-InP multiple-quantum-well lasers," *IEEE J. Quantum Electron.*, vol. 32, no. 12, pp. 2133–2138, Dec. 1996.

[4] T. R. Chen, P. C. Chen, J. Ungar, M. A. Newkirk, S. Oh, and N. Bar-Chaim, "Low-threshold and high-temperature operation of InGaAlAs-InP lasers," *IEEE Photon. Technol. Lett.*, vol. 9, no. 1, pp. 17–18, Jan. 1997.

[5] K. Takemasa, M. Kubota, T. Munakata, and H. Wada, "1.3μm AlGaInAs buried-heterostructure lasers," *IEEE Photon. Technol. Lett.*, vol. 11, no. 8, pp. 949–951, Aug. 1999.

[6] S. R. Selmic, T.-M. Chou, J. Sih, J. B. Kirk, A. Mantle, J. K. Butler, D. Bour, and G. A. Evans, "Design and characterization of 1.3-μm AlGaInAs-InP multiple-quantum-well lasers," *IEEE J. Sel. Topics Quantum Electron.*, vol. 7, no. 2, pp. 340–349, Mar.–Apr. 2001.

[7] J. Decobert, N. Lagay, C. Cuisin, B. Dagens, B. Thedrez, and F. Laruelle, "MOVPE growth of AlGaInAs-InP highly tensile-strained MQWs for 1.3 μm low-threshold lasers," *J. Crystal Growth*, vol. 272, nos. 1–4, pp. 543–548, Dec. 2004.

[8] M. Allovon and M. Quillec, "Interest in AlGaInAs on InP for opto-electronic applications," *IEE Proc. J Optoelectron.*, vol. 139, no. 2, pp. 148–152, Apr. 1992.

[9] J. C. L. Yong, J. M. Rorison, and I. H. White, "1.3-μm quantum-well InGaAsP, AlGaInAs, and InGaAsN laser material gain: A theoretical study," *IEEE J. Quantum Electron.*, vol. 38, no. 12, pp. 1553–1564, Dec. 2002.

[10] T. J. Houle, J. C. L. Yong, C. M. Marinelli, S. Yu, J. M. Rorison, I. H. White, J. K. White, A. J. SpringThorpe, and B. Garrett, "Characterization of the temperature sensitivity of gain and recombination mechanisms in 1.3-μm AlGaInAs MQW lasers," *IEEE J. Quantum Electron.*, vol. 41, no. 2, pp. 132–139, Feb. 2005.

[11] B. Stegmuller, B. Borchert, and R. Gessner, "1.57 μm strained-layer quantum-well GaInAlAs ridge-waveguide laser diodes with high temperature (130 °C) and ultrahigh speed (17 GHz) performance," *IEEE Photon. Technol. Lett.*, vol. 5, no. 6, pp. 597–599, Jun. 1993.

[12] N. Ikoma, T. Kawahara, N. Kaida, M. Murata, A. Moto, and T. Nakabayashi, "Highly reliable AlGaInAs buried heterostructure lasers for uncooled 10 Gb/s direct modulation," in *Proc. Tech. Dig. Opt. Fiber Commun. Conf.*, Anaheim, CA, Mar. 2005, pp. 1–3.

[13] T. Nakamura, T. Okuda, R. Kobayashi, Y. Muroya, K. Tsuruoka, Y. Ohsawa, T. Tsukuda, and S. Ishikawa, "1.3-μm AlGaInAs strain compensated MQW-buried-heterostructure lasers for uncooled 10-Gb/s operation," *IEEE J. Sel. Topics Quantum Electron.*, vol. 11, no. 1, pp. 141–148, Jan.–Feb. 2005.

[14] K. Yashiki, T. Kato, H. Chida, K. Tsuruoka, R. Kobayashi, S. Sudo, K. Sato, and K. Kudo, "10-Gb/s 23-km penalty-free operation of 1310-nm uncooled EML with semi-insulating BH structure," *IEEE Photon. Technol. Lett.*, vol. 18, no. 1, pp. 109–111, Jan. 2006.

[15] K. Nakahara, T. Tsuchiya, T. Kitatani, K. Shinoda, T. Taniguchi, T. Kikawa, M. Aoki, and M. Mukaikubo, "40-Gb/s direct modulation with high extinction ratio operation of 1.3-μm InGaAlAs multiquantum well ridge waveguide distributed feedback lasers," *IEEE Photon. Tecnol. Lett.*, vol. 19, no. 19, pp. 1436–1438, Oct. 2007.

[16] K. Otsubo, M. Matsuda, K. Takada, S. Okumura, M. Ekawa, H. Tanaka, S. Ide, K. Mori, and T. Yamamoto, "Uncooled 25 Gb/s direct modulation of semi-insulating buried-heterostructure 1.3 μm AlGaInAs quantum-well DFB lasers," *Electron. Lett.*, vol. 44, no. 10, pp. 631–632, May 2008.

[17] T. Fujisawa, M. Arai, N. Fujiwara, W. Kobayashi, T. Tadokoro, K. Tsuzuki, Y. Akage, R. Iga, T. Yamanaka, and F. Kano, "25 Gb/s 1.3 μm InGaAlAs-based electroabsorption modulator integrated with DFB laser for metro-area (40 km) 100 Gb/s Ethernet system," *Electron. Lett.*, vol. 45, no. 17, pp. 900–902, Aug. 2009.

[18] Y. Yoshida, H. Watanabe, K. Shibata, A. Takemoto, and H. Higuchi, "Analysis of characteristic temperature for InGaAsP BH lasers with p-n-p-n blocking layers using two-dimensional device simulator," *IEEE J. Quantum Electron.*, vol. 34, no. 7, pp. 1257–1262, Jul. 1998.

[19] R. Gessner, A. Dobbinson, A. Miler, J. Rieger, and E. Veuhoff, "Fabrication of AlGaInAs and GaInAsP buried heterostructure lasers by in situ etching," *J. Crystal Growth*, vol. 248, pp. 426–430, Feb. 2003.

[20] S. Codato, R. Campi, C. Rigo, and A. Stano, "Ga assisted in situ etching of AlGaInAs and InGaAsP multiquantum well structures using tertiarybutylchloride," *J. Crystal Growth*, vol. 282, nos. 1–2, pp. 7–17, Aug. 2005.

[21] W. Feng, J. Q. Pan, L. F. Wang, J. Bian, B. J. Wang, F. Zhou, X. An, L. J. Zhao, H. L. Zhu, and W. Wang, "Fabrication of InGaAlAs MQW buried heterostructure lasers by narrow stripe selective MOVPE," *J. Phys. D, Appl. Phys.*, vol. 40, no. 2, pp. 361–365, Jan. 2007.

[22] T. Tanbun-Ek, S. N. G. Chu, P. W. Wisk, R. Pawelek, A. M. Sergent, J. Minch, E. Young, and S. L. Chuang, "High performance buried heterostructure 1.55 μm wavelength AlGaInAs/InP multiple quantum well lasers grown entirely by MOVPE technique," in *Proc. 10th Int. Conf. Indium Phosphide Rel. Mater.*, Tsukuba, Japan, May 1998, pp. 702–705.

[23] Y. Takino, M. Shirao, T. Sato, N. Nishiyama, T. Amemiya, and S. Arai, "Regrowth interface quality dependence on thermal cleaning of AlGaInAs/InP buried-heterostructure lasers," *Jpn. J. Appl. Phys.*, vol. 50, no. 7, pp. 070203-1–070203-3, Jul. 2011.

[24] N. Sato, Y. Takino, M. Shirao, T. Sato, N. Nishiyama, and S. Arai, "Effect of thermal cleaning on regrowth interface quality of AlGaInAs/InP buried heterostructure lasers," presented at the 38th International Symposium on Compound Semiconductors, Berlin, Germany, May 2011.

[25] B. E. Maile, A. Forchel, R. Germann, and D. Grotzmacher, "Impact of sidewall recombination on the quantum efficiency of dry etched InGaAs/InP semiconductor wires," *Appl. Phys. Lett.*, vol. 54, no. 16, pp. 1552–1554, Apr. 1989.

[26] M. Tamura, Y. Nagashima, K. Kudo, K.-C. Shin, S. Tamura, A. Ubukata, and S. Arai, "Surface damage in GaInAs/GaInAsP/InP wire structures prepared by substrate-potential-controlled reactive ion beam etching," *Jpn. J. Appl. Phys.*, vol. 34, no. 6A, pp. 3307–3308, Jun. 1995.

[27] M. Tamura, T. Ando, N. Nunoya, S. Tamura, S. Arai, and G. U. Bacher, "Estimation of sidewall nonradiative recombination in GaInAsP/InP wire structures fabricated by low energy electron-cyclotron-resonance reactive-ion-beam-etching," *Jpn. J. Appl. Phys.*, vol. 37, no. 6A, pp. 3576–3584, Jun. 1998.

[28] M. Tamura, T. Kojima, T. Ando, N. Nunoya, S. Tamura, and S. Arai, "Sidewall recombination velocity in GaInAsP/InP quantum-well lasers with wire-like active region fabricated by wet-chemical etching and organo-metallic vapor-phase-epitaxial regrowth," *Jpn. J. Appl. Phys.*, vol. 37, no. 12A, pp. 6569–6574, Oct. 1998.

[29] D. B. Wittry and D. F. Kyser, "Measurement of diffusion lengths in direct-gap semiconductors by electron-beam excitation," *J. Appl. Phys.*, vol. 38, no. 1, pp. 375–382, Jan. 1967.

[30] P. Abraham, A. Bekkaoui, V. Soulière, J. Bouix, and Y. Monteil, "Thermal decomposition studies of group V hydrides," *J. Crystal Growth*, vol. 107, nos. 1–4, pp. 26–31, Jan. 1991.

Yuta Takino was born in Gunma, Japan, in 1987. He received the B.E. and M.E. degrees from the Tokyo Institute of Technology, Tokyo, Japan, in 2009 and 2011, respectively.

He joined Nippon Telegraph and Telephone East Corporation, Tokyo, in 2011. His current research interests include organometallic vapor phase epitaxy technique and the fabrication process of the buried heterostructure-laser in the AlGaInAs materials system.

Mr. Takino is a member of the Japan Society of Applied Physics.

Mizuki Shirao (S'08–M'12) received the B.E., M.E., and Ph.D. degrees in electrical and electronic engineering from the Tokyo Institute of Technology, Tokyo, Japan, in 2007, 2009, and 2011, respectively.

He joined Mitsubishi Electric Corporation, Ltd., Tokyo, Japan, in 2011. His current research interests include long-wavelength transistor lasers and THz modulation by optical signals.

Dr. Shirao is a member of the Japan Society of Applied Physics.

Noriaki Sato was born in Shizuoka, Japan, in 1988. He received the B.E. degree from the Tokyo Institute of Technology, Tokyo, Japan, in 2011. He is currently pursuing the Masters degree with the same university.

His current research interests include the improvement of buried heterostructure laser characteristics in the AlGaInAs material system.

Mr. Sato is a member of the Japan Society of Applied Physics.

Takashi Sato was born in Ibaraki, Japan, in 1987. He received the B.E. and M.E. degrees from the Tokyo Institute of Technology, Tokyo, Japan, in 2010 and 2012, respectively.

He joined Nippon Telegraph and Telephone East Corporation, Tokyo, in 2012. His current research interests include fabrication processes of long-wavelength transistor lasers.

Mr. Sato is a member of the Japan Society of Applied Physics.

Tomohiro Amemiya (S'06–M'09) received the B.S., M.S., and Ph.D. degrees in electronic engineering from the University of Tokyo, Tokyo, Japan, in 2004, 2006, and 2009, respectively.

He was with the Quantum Electronics Research Center, Tokyo Institute of Technology, Tokyo, in 2009, where he is currently an Assistant Professor. His current research interests include physics of semiconductor light-controlling devices, metamaterials for optical frequency, magneto-optical devices, and the processing technologies for the fabrication of these devices.

Dr. Amemiya is a member of the Optical Society of America, the American Physical Society, and the Japan Society of Applied Physics. He was the recipient of the IEEE Photonics Society Annual Student Paper Award in 2007 and the IEEE Photonics Society Graduate Student Fellowships in 2008.

Nobuhiko Nishiyama (M'01–SM'07) was born in Yamaguchi, Japan, in 1974. He received the B.E., M.E., and Ph.D. degrees from the Tokyo Institute of Technology, Tokyo, Japan, in 1997, 1999, and 2001, respectively. He demonstrated single-mode 0.98- and 1.1-μm vertical-cavity surface-emitting laser (VCSEL) arrays with stable polarization using misoriented substrates for high-speed optical networks as well as metalorganic chemical vapor deposition-grown GaInNAs VCSELs, during his Ph.D. work.

He joined Corning Inc., Corning, NY, in 2001, and the Semiconductor Technology Research Group. At Corning Inc., he worked on several subjects including short-wavelength lasers, 1060-nm DFB/DBR lasers, and long-wavelength InP-based VCSELs, demonstrating state-of-the-art results, such as 10-Gb/s isolator-free and high-temperature operation of long-wavelength VCSELs. He has been an Associate Professor with the Tokyo Institute of Technology since 2006. His current research interests include laser transistors, silicon-photonics, III–V silicon hybrid optical devices, and THz-optical signal conversions involving optics-electronics-radio integration circuits.

Dr. Nishiyama is a member of the Japan Society of Applied Physics, the Institute of Electronics, Information and Communication Engineers (IEICE), and the IEEE Photonics Society. He received the Excellent Paper Award from the IEICE of Japan in 2001 and the Young Scientists Prize in the Commendation for Science and Technology from the Minister of Education, Culture, Sports, Science, and Technology in 2009.

Shigehisa Arai (M'83–SM'06–F'10) was born in Kanagawa, Japan, in 1953. He received the B.E., M.E., and D.E. degrees in electronics from the Tokyo Institute of Technology, Tokyo, Japan, in 1977, 1979, and 1982, respectively. He demonstrated room-temperature CW operations of 1.11– to 1.67-μm long-wavelength lasers fabricated by liquid-phase-epitaxy as well as their single-mode operation under rapid direct modulation during his Ph.D. work.

He joined the Department of Physical Electronics, Tokyo Institute of Technology, as a Research Associate in 1982, and joined AT&T Bell Laboratories, Holmdel, NJ, as a Visiting Researcher from 1983 to 1984, on leave from the Tokyo Institute of Technology. Then, he became a Lecturer in 1984, an Associate Professor in 1987, and a Professor with the Research Center for Quantum Effect Electronics and the Department of Electrical and Electronic Engineering in 1994. He has been a Professor with the Quantum Nanoelectronics Research Center, Tokyo Institute of Technology, since 2004. His current research interests include photonic integrated devices, such as dynamic-single-mode and wavelength-tunable semiconductor lasers, semiconductor optical amplifiers, optical switches/modulators, studies on low-damage and cost-effective processing technologies of ultrafine structures for high-performance lasers, and photonic integrated circuits on silicon platforms.

Dr. Arai is a member of the Optical Society of America. He is a fellow of the Institute of Electronics, Information and Communication Engineers (IEICE) and the Japan Society of Applied Physics. He received an Excellent Paper Award at IEICE of Japan in 1988, the Michael Lunn Memorial Award from the Indium Phosphide and Related Materials Conference in 2000, Prizes for Science and Technology, including a Commendation for Science and Technology from the Minister of Education, Culture, Sports, Science, and Technology in 2008, the Electronics Society Award, and the Achievement Award from IEICE in 2008 and 2011, respectively.